Journal of Mines, Metals and Fuels, *73(3): 663-679; 2025. DOI: 10.18311/jmmf/2025/47408*

Print ISSN : 0022-2755

Journal of Mines, Metals and Fuels

Contents available at: *www.informaticsjournals.co.in/index.php/jmmf*

High Temperature Wear Performance of Micron and Nano Coatings by Thermal Spray Technique-A Critical Review

C. R. Raghavendra[1], Shiddalingayya Mathad[1,2], A. M. Satish[3], Manjunath Vatnalmath[4], V. Auradi[4], K. C. Vishwanath[5]*, V. Bharath[6], K. Annapoorna[6], Nagaraj Namdev[7], Fazil Nalband[8] and Madeva Nagaral[9]

[1]Department of Mechanical Engineering, Government Engineering College, Haveri (Visvesvaraya Technological University, Belagavi), Haveri - 581110, Karnataka, India

[2]Department of Mechanical Engineering, Government Polytechnic College, Hanagal - 581104, Karnataka, India

[3]Department of Mechanical Engineering, S J Government Polytechnic, Bengaluru - 560001 Karnataka, India

[4]Department of Mechanical Engineering, Siddaganga Institute of Technology, Tumakuru - 572103, Karnataka, India

[5]Department of Robotics and Automation, Rajarajeswari College of Engineering, Bangalore - 560074, Karnataka, India; drvishwanathkc@gmail.com

[6]Department of Mechanical Engineering, RNS Institute of Technology, Bengaluru - 560098, Karnataka, India

[7]Department of Mechanical Engineering, APS Polytechnic, Bangalore - 560082, Karnataka, India

[8]Department of Mechanical Engineering, Ballari Institute of Technology and Management, Ballari - 583104, Karnataka, India

[9]Aircraft Research and Design Centre, Hindustan Aeronautics Limited, Bangalore - 560037, Karnataka, India

Abstract

The main objective of this review is to highlight the need for multipurpose materials by surface engineering approach towards high-temperature wear applications. In this context, the demand for surface coating is increasing in the field of automobile and aerospace applications. The high-temperature wear-resistant property materials by micron and nanoparticle coating have provided a new window for increased functional properties for the conventional substrate surfaces. There are many coating techniques available for micro/nano coatings. Every coating technique has its own advantages and disadvantages. The use of these coating techniques depends on various intrinsic and extrinsic factors of coating material, substrate material used and coating application. The thermal spray technique allows hard particles with various sizes and characteristics of secondary phase particles to be coated effectively. This critical review majorly deals with thermal barrier coating applied onto the various substrates used in high-temperature applications. Furthermore, the microstructure and composition of the coatings are highlighted. The different types of anti-corrosive and wear-resistance coating characteristics are described.

Keywords: *Coatings, High Temperature, Submicron Particles, Thermal Spray, Wear*

**Author for correspondence*

1.0 Introduction

Many mechanical parts are exposed to different working environments. Oxidation, abrasion, corrosion, and wear are typical degradation phenomena that the parts are repeatedly subjected to. Industries such as automobiles, aerospace, marine, and biomedical will have a greater impact on these phenomena[1,2].

The parts having relative motion will experience gradual degradation of the surface due to different kinds of wear that depends on the surrounding media and the properties of both parts[1]. The performance and life of the material were remarkably reduced due to severe wear. It is more challenging to reduce friction in metal-to-metal contact mating parts. Surface roughness and hardness are the main factors that greatly influence the parts' friction and wear. Surface roughness is the function of the machining process and can be achieved by super finishing operations. Hardness is a material's mechanical property and will adversely affect other properties when it increases inherently. Therefore, it is essential to have different properties like hardness in case and strength at the core to withstand friction and loads. Core material properties are inherent properties and not possible to alter. Case properties are altered by using surface treatment processes. Surface treatment processes play an important role in achieving the required performance and life of material when it undergoes relative motion with mating parts. Surface treatments are of two types, one by heat treatment process through which case of the base material properties are altered by heating and cooling the parts at a specified rate. The second type is by coating technique in which the surface of the base material is covered with materials having required properties by different methods. Finger seal is a kind of seal used in aero engines, tuyeres used in furnaces, most of the parts in power generating industries, cutting tools, valves, and jet nozzles are some of the practical examples that will experience erosion, abrasion, and thermal fatigue[3]. High temperature-resistant coatings will support an increase in the surface properties to extend the life of the components. Research has been done to overcome these issues and invented some high temperature wear resistant coatings in past years[3]. There are many kinds of surface coating techniques, depending on the type of base material called substrate, coating material, required properties, operating condition, and load. In the present paper, extensive review and analysis have been done with reference to the high-temperature wear performance of the composite coating and coating details by the high-velocity oxyfuel method.

2.0 Coating Techniques

Coating technologies can cause a performance that may not be achievable only with the base material to provide wear resistance in many engineering components. The process of coating will provide protection to the components or the surface which are exposed to harsh and corrosive environments in a variety of engineering fields like aerospace, automotive industries to biomedical devices like tiny implants inside the human body[4]. The scope of the surface alteration and coating is to alter the characteristics by various methods viz., bulk and hard coatings, atomic level and particulate type deposition and many more[1].

Coating techniques are available in many ways due to the enormous range of applications and requirements in different areas. These techniques consist of many parameters that will give many results regarding microstructure, efficiency, durability, and suitability. Though many coating methods are practically useful, practical applications depending on preferred functional properties, wear and corrosion protection have major importance[4,5].

Among all surface coating techniques, thermal spray is more special as it gives rough surface quality formed during the spraying and a reliable method of wear and corrosion coatings[4]. In the subsequent decades, scientists made many varieties of thermal spray methods available to coat hard materials. Few of them practically used in earlier days are found to be High Velocity Oxygen Fuel (HVOF), plasma, flame, arc spray techniques have been progressively industrialized to coat different metal alloys to serve every category of requirements engineering applications[6,7].

3.0 Different Thermal Spraying Techniques

1) Flame Spraying or Combustion Flame Spraying.
a) Powder Flame Spraying.
b) Wire Fame Spraying.

2) Electric Arc Spraying (EAS).
3) Atmospheric Plasma Spraying (APS).
a) Vacuum Plasma Spraying (VPS) or Low-Pressure Plasma Spraying (LLPS).
b) Transferred Arc Plasma Spraying.
4) Detonation Gun Spraying (DGS).
5) High Velocity-Oxy-Fuel Spraying (HVOF).
6) Controlled Atmospheric Plasma Spraying (CAPS).

All the above thermal spray techniques are established to heat and accelerate the particles to get a high temperature and high-velocity jet of molten state particles. The molten state particles are forced to strike onto the surface of the substrate. The thermal spray coating is initially deposited by the uninterrupted strike of molten particles trailed by the spreading of droplets. Further cooling and solidification take place rapidly and get the coarse surface. The adhesion and cohesion of the adjacent splats during the coating play an important role in deciding the quality of coating[6]. The coating material can be in many forms, mainly powder, wire, rod or even in molten state[8-10].

More interest have been taken to achieve realistic coatings by thermal spraying methods[11,12]. HVOF thermal spraying technique is treated as the best techniques to produce hard material coatings, because of many technical processes involved in such as more flame velocity, less flame temperature, decarburization prevention and minimum formation of harmful products[3,13,14].

Thermal spray techniques satisfy the restricted chemical interactions with the substrate materials, in addition it will avoid reactions during the process[15]. HVOF method of coating process is industrially recognized more due to its flexibility in dense production of particles and for their low oxide cermet deposition[16,17].

4.0 High-Velocity Oxy-Fuel Coating

High velocity oxy fuel coating is a thermal spray technique in which propane, acetylene, hydrogen, kerosene are used as fuel in the form of liquid or gas along with oxygen. Combustion of fuel with the presence of oxygen is conducted in the combustion chamber. After mixture is burnt, hot gas generated with a high temperature and pressure. The hot gas is passed through a nozzle to increase the kinetic energy at a velocity of about 1000 m/s. About 2500°C to 3100°C temperature generated in the process depending on the oxygen and type of fuel used[18] The primary and secondary coating material can be of the powder, rod and/or wire form which are to flow into the hot gas stream which melts and forced to strike the base material with higher velocity. Some of the advantages in this process are less number of oxides due to inert shrouding and reduces flight time due to high speeds of particles, very less time to have oxidation reaction, high thermal and kinetic energy will lead to strong bonding and dense and thick coated surfaces are possible to get by HVOF process[8,19,20].

HVOF process has superior coating characteristics. They comprise high bonding strength, dense structure, very less number of pores and high surface hardness[1]. Compared to other methods of thermal spray studies HVOF, plasma, detonation gun coatings shows the advantages in terms of tribological properties, density, cohesive strength[21,22]. One more advantage of HVOF process is providing multilayer coatings on the surface. Non-conductive materials like ceramics and polymers are be able coat on metallic substrates[4].

The study confirmed that HVOF is an applicable and cost-effective technique to coat with very less porosity to resist wear at high temperature and corrosion. Excellent wear resistance property of HVOF thermal spraying technique used to machine cutters, mining tools and wear machine parts[23–27]. Many researchers reported that, bimodal powder (mixer of nano sized and micro sized) WC particles are coated by HVOF technology can enhance wear resistance in combination with hardness and toughness and also cost effective[28,29]. Thermal sprayed coatings create protective layers to protect components used in gas turbines and aircraft engines from hot corrosion and high temperature oxidation[30,31]. One more property of HVOF coatings is that, after spraying the powder feedstock can be able to retain the nano-scale structure[30,32–34].

In the following years the increase in energy requirement with environmental constraints forcing the engineering industries to invent more efficient and harmless materials to use in power generation[35–37]. To safeguard against wear and high temperature corrosion, Al_2O_3 and NiAl cermet coating are better choice[38]. TiB_2-Ni composites are most preferred to produce corrosion and wear resistance on the interface surfaces in metal-to-

metal contact parts. Conventionally thermal spraying and laser cladding method are preferred to coat TiB_2-Ni[39]. The great advantage of high energy, high temperature and good efficiency of HVOF method is appropriate to produce efficient coating with high bonding strength, hardness and density[40–43].

5.0 HVOF Process Parameters

The coating by HVOF is mainly influenced by the optimum parameters' selections. The quality and the function of the coating significantly depend on coating parameters which are needed to selected appropriately. The process parameters of HVOF are namely: oxygen flow rate, flow rate of liquid/gas fuel, distance between spray nozzle and substrate, coating powder flow rate, shape of the powder, size of the particle viz., micro and nano, velocity with which the particle strikes the target, temperature attained by the particle melting during the coating, angle of impact of the particles on to the target, and preheat temperature of the base metal/target[44]. Though the parameters of coating method are entirely self-regulating on variables, whilst outcomes dependent variables. The outcomes of coatings are in terms of hardness, coating thickness, respective coating porosity, wear, toughness of the coating, corrosion resistance and oxidation[8,45].

Many researchers have extensively optimized the parameters related to HVOF. Vignesh *et al.* worked on optimizing spray parameters mainly to attain less porosity and high hardness[45]. Among different parameters, the oxygen flow rate to be the forceful factor which controls the porosity and hardness of the coating. Thermal and kinetic energy are the main two factors which influence porosity. Less thermal energy and high kinetic energy will give minimum porous coatings. Proper selection of oxygen and fuel ratio greatly influences stream velocity and flame temperature. At low temperature, the quantity of free oxygen becomes low and at the same time flame temperature increases. The increase in air/fuel ratio makes flame heavier and thereby coating particles carrying capacity decreases which results in kinetic energy. The study shows that controlling oxygen/fuel ratio is incredibly significant. Wang *et al.*[8] made a study on iron-based amorphous solid and observed that the decrease in O/F ratio results in higher powder feed with respect to the time and also porosity due to entrapment of some portion of un-melted particles.

Rukhande *et al.*[19] used the HVOF technique to coat on SS316L substrate material. The benefit chromium substance in the NiCrBSiFe composite powder is found to resist high-temperature corrosion, and boron helps to reduce the melting temperature of the composite. The higher hardness possessed by the chromium and boron particles has resulted in higher coating hardness. Self-fluxing property can be enhanced by silicon. The Stainless steel (316L) substrates were prepared by surface blasting with 5 bar air pressure. The blasting angle was maintained at 90° to the target in a pressure blasting machine, which was used to spray the coating. The calculated proportion

Table 1. HVOF coating parameter for NiCrBSiFe coating on SS316L[19]

Parameter	HVOF Spraying Process
Gas Flow Rate	240 LPM (Oxygen), 550 LPM (Air)
Feed Rate of Powder	45 gm/min
Particle Temperature	2210 °C
Particle Velocity	534 m/s
Deposition Efficiency	65%
Stand-off Distance	150 mm

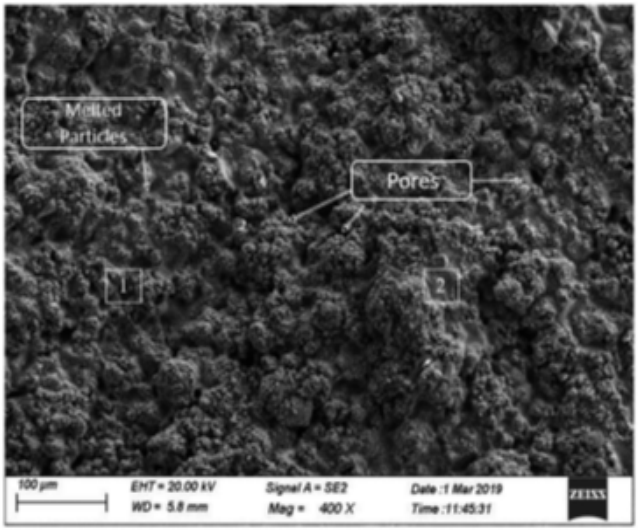


Figure 1. Surface morphology of sprayed coating surface[19].

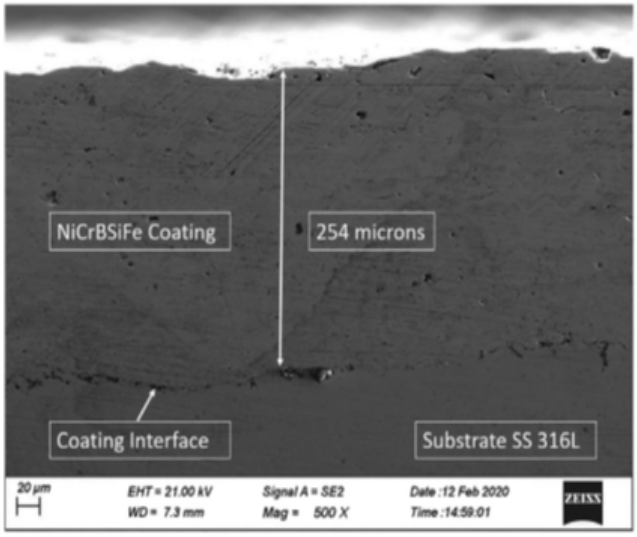


Figure 2. Cross section of NiCrBSiFe coated on SS316L[19].

of fuel (LPG) and oxygen are made to burn with 10 kg/cm^2 oxygen pressure. The processing parameters are as per Table 1 for the deposition using the HVOF process.

Figure 1 shows the coated surface SEM images sprayed by HVOF process. A metallurgical bonding takes place with base metal surface by the molten composite powder during the process[46,47]. Maximum flight velocity during the HVOF process will lead to minimum oxidation and less oxide inclusion while coating. Due to this reason more smooth, dense, crackled, wear resistant and corrosion resistant coatings were produced. Like other thermal spray processes, some splats, partially melted, globules and few voids were observed. Also high density and small pores coating were met by HVOF[19].

Figure 2 shows the cross-section image of the coating interface. Coating thickness varied from 250 microns to 300 microns with HVOF coating process[19].

Hong *et al.*[3] used steel (AISI1045) plates were used as the substrate. Nano-structured WC-CoCr powder with a small proportion of Cr 4% by wt, Co 10 % by wt, C 5.3% by wt, W 80.7% by wt was used as coating material. 100 to 500nm size particles are used, and 5–45 µm agglomerated distribution. The particles are almost spherical in shape[3]. Table 2 gives the nanostructured WC-CoCr coating hardness results for two loading conditions. Vickers hardness data at 100g and 300g indentation load mono modal distribution is plotted by using Weibull, revealing unique characteristics for both loads. For lower indentation load, high hardness with relatively wide ranges is detected. This may be due to the existence of defects like microcracks, and pores viewed in different directions. For higher indentation load, the indentations cover larger areas. This may be due to the microstructural defects which lead to a reduction in mechanical[3]. Based on the image provided, here is the data organized in a table format which is shown in Table 2.

6.0 Tribological Behaviour of the Coating

Figure 3 shows the change in friction coefficient with the sliding time at different temperature conditions. Coefficients of friction indicate the adhesive wear resistance, lower coefficients of friction means higher wear resistance[48]. There are two typical friction systems for coatings, viz., running in period and/or steady-state period. It is observed in the graph that the coefficient of friction curves has more deviations when evaluated

Table 2. Results of Weibull distribution of WC-CoCr nanostructured coating[3]

Load (g)	Hardness range		m	n	Average Hardness, HV
	HV	ln HV			
100	983-1351	6.89-7.20	14.200	50	1200
300	906-992	6.84-6.90	28.689	14	952
	1010-1193	6.92-7.11	13.485	36	1100
	(906-1193)	(6.84-7.11)		(50)	(1064)

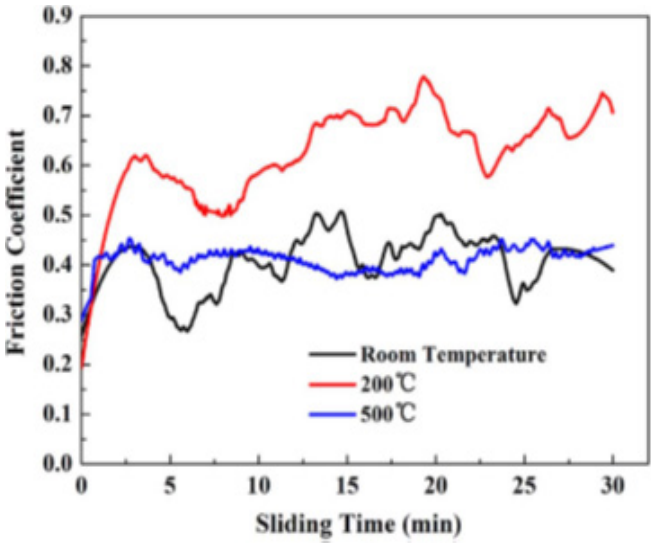
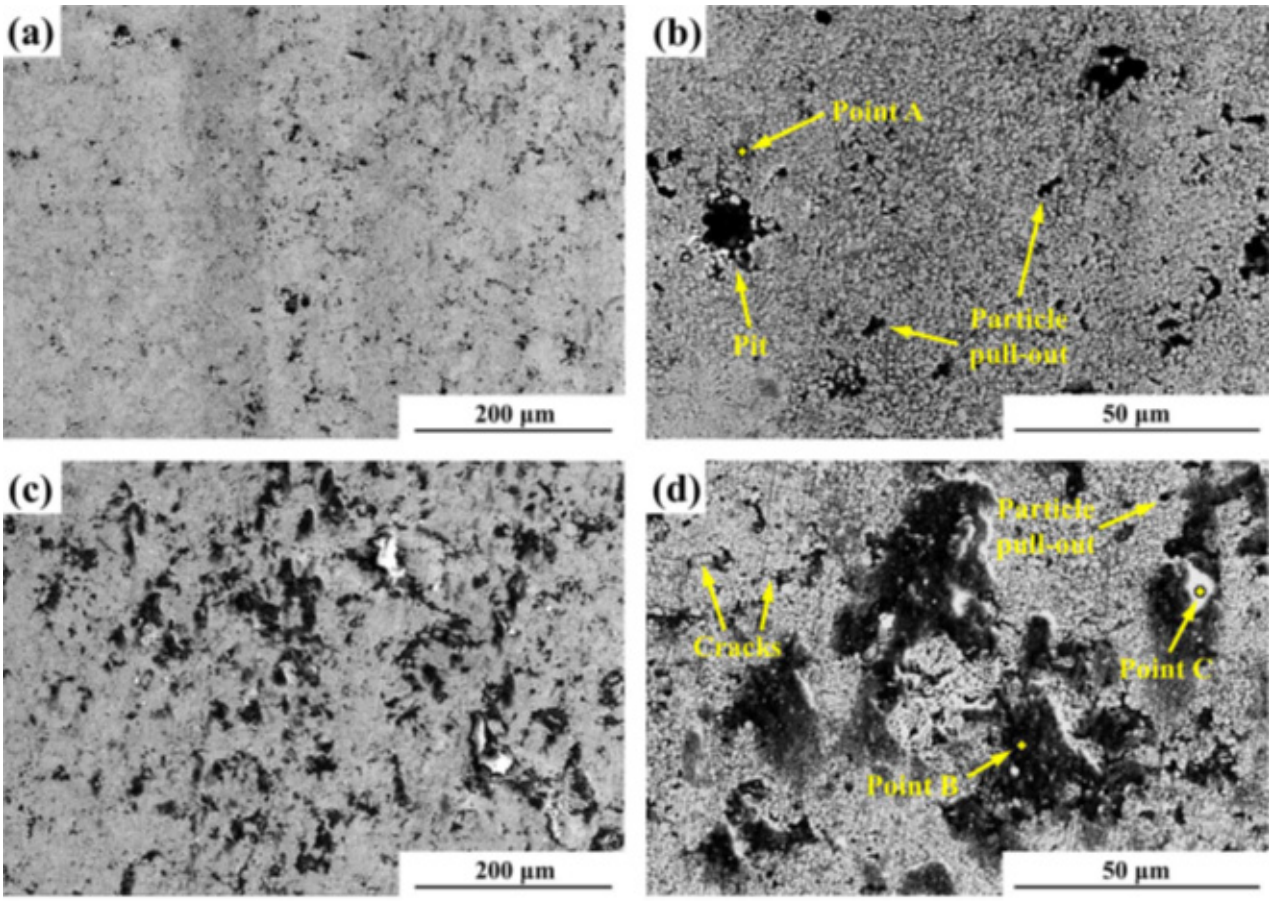


Figure 3. Friction Coefficients versus sliding time at room temperature, 200°C and (Al_2O_3 as counterpart, 50N load, 0.9m/s sliding velocity)[3].

at different temperature conditions. Variation of the coefficient of friction at 500°C is lesser than at room temperature and 200°C. This variation is because of the formation of the high amount of oxide films having a lubrication effect because of tiny debris on the worm surface at 500°C[3].

7.0 Surface Morphology and Coating Composition

Figure 4 shows the images of the worn-out surface of the coating. Al_2O_3 ball is used as a counterpart against the coated surface under the load 50N. The morphological results revealed a smooth, worn surface at the surrounding temperature for a period of 180 sec (Figure. 4(a)). Some tiny pits and supplements of carbide particles are found, showing that minor material deletion occurs when the wear test is done at room temperature, as shown in Figure 4(b). The EDS analysis with wt.% at point A (Figure 4(b))



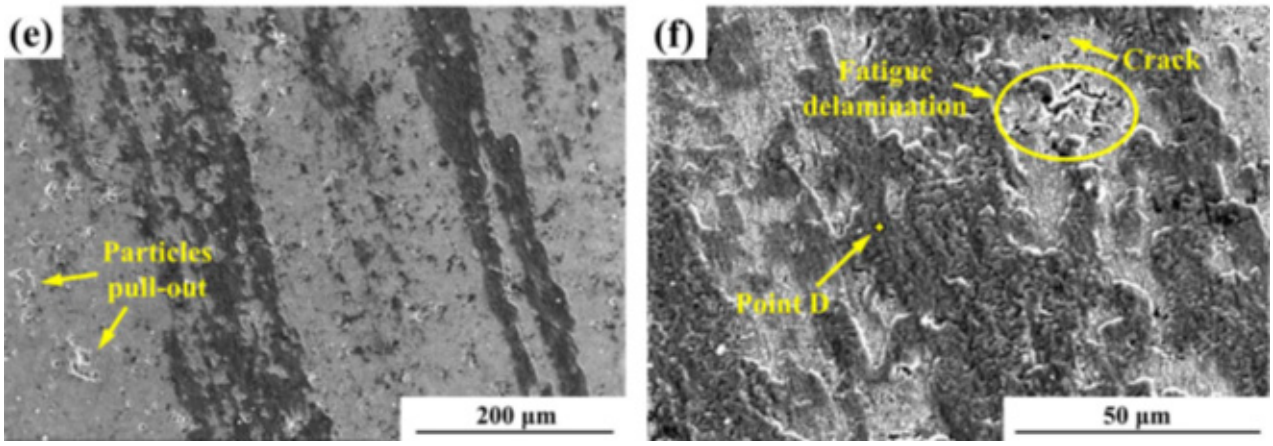


Figure 4. SEM morphologies of worn-out surfaces of WC-CoCr nanostructured coatings evaluated at various temperature[3].

Table 3. Deposition parameters WC-10Co-4Cr coating[48]

Parameters	Operating range
Stand-off distance, mm	360
Powder feed g/min	45
Oxygen supply, l/min	850
Carrier gas supply, l/min Nitrogen	12
Fuel supply, ml/min	330
Water supply, Limin Coolant	30-32
Combustion pressure, bar	6-6.5

discloses the presence of Co, W and O, representing that some oxides are produced. Figure 4(c) shows that as the temperature increases to 200°C, the worn-out surface becomes a rough region, which is observed in point B in Figure 4(d).

Sapate *et al.*[49] used EN-24 steel as a substrate and WC-10Co-4Cr composite having 86%-WC, 10%-Co, 4%-Cr proportions with sintered and agglomerated powder used for coating. The powder particles with sizes 45 microns to 15 microns were spherical in shape. 150, 300 and 450 lm coating thickness specimens were used for characterization. Before deposition, all substrates are cleaned by grit blasting and ultrasonic methods. Table 3 gives the deposition parameters details.

8.0 Microstructure and Phase Analysis

Figure 5 (a)-(d) illustrates SEM morphologies of the coating surface. Brighter areas identify the WC grains, whereas WC surrounds Co grains with dark areas. The percentage of porosity corresponding to the thickness of the coating was found to be 1.10 ± 0.07% (150), 0.91 ±0.06%(300m) and 1.30 ± 0.09%(450lm). Point-1 and point-2 EDS spectra are shown in Figure 5(e) and (f). Peaks showed EDS spectra of tungsten. Chromium and cobalt are shown with the darker areas having major peaks in Figure 6(f), revealing the chromium and cobalt binder phases. Coating with 450lm thickness exhibits decarburization of WC particles, and they solidify easily at the circumference of WC particles because of their small size[49].

9.0 Mechanical Properties

Table 4 gives the results of elasticity, residual stress, and bonding strength for different coating thickness. The modulus of elasticity shows the highest for 300lm and lowest value for 450lm coating. High porosity and less adhesion strength occurs coating thicknesses is increased

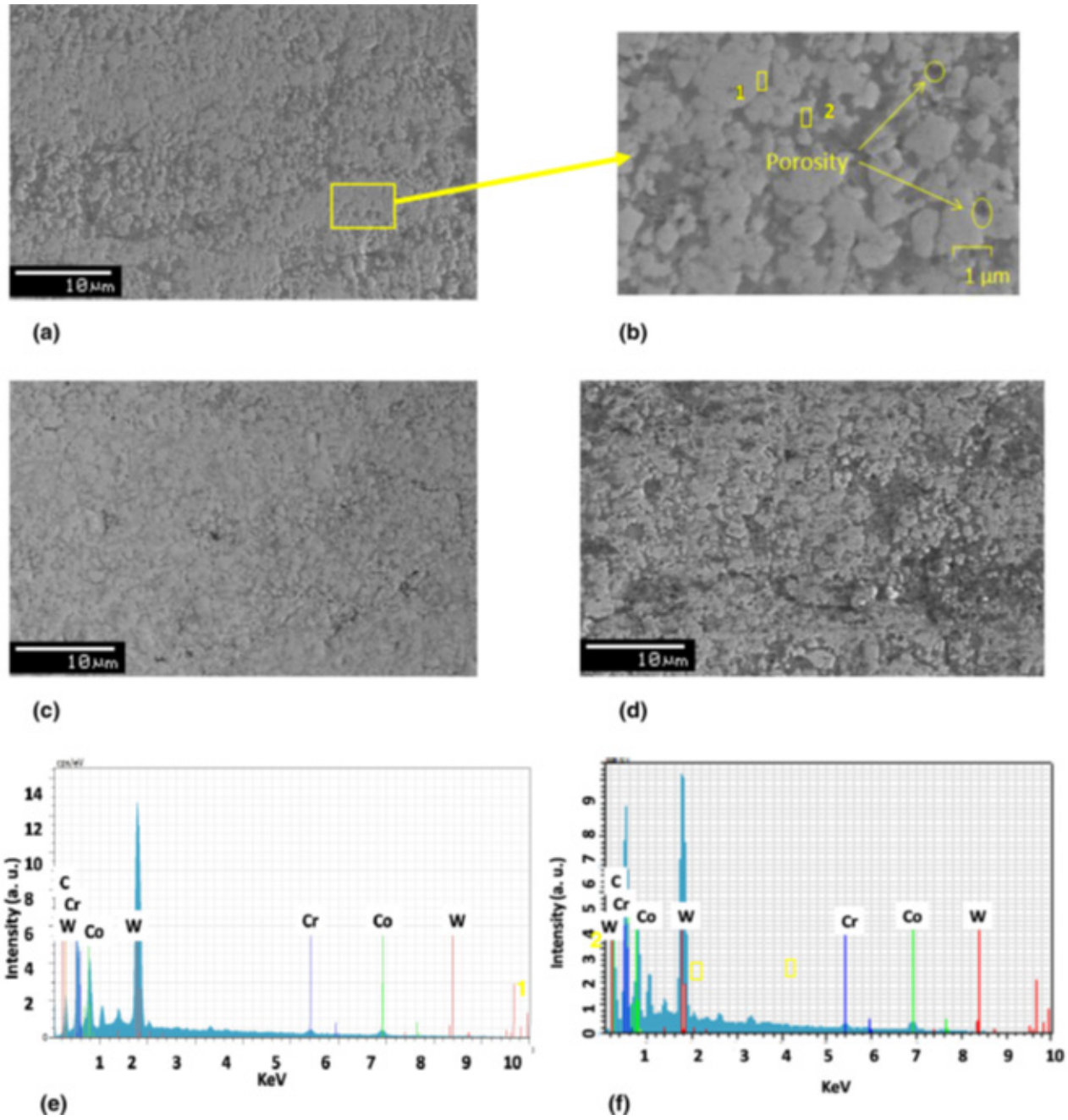


Figure 5. **(a)** SEM image of 150 micron coating; **(b)** Enarged details square area pointed in (a); **(c)** SEM images of 300micron; **(d)** SEM images of 450micron; **(e)** EDS at point 1 pointed in (b); **(f)** EDS at point 2 pointed in (b)[49].

Table 4. WC-10Co-4Cr composite coating results: Elastic modulus, Residual stress, and Bond strength[49]

Sr. no.	Coating thickness µm	Elastic modulus GPa	Residual stress MPa	Nature of stress	Bond strength, MPa
1	150	239.10± 130	434.41±2.5	Compressive	75.38±3.1
2	300	24270± 17.0	269.27±2.1	Compressive	73.02±1.8
3	450	217.50± 14.0	203.34±3.4	Compressive	70.65±2.4

and decreases modulus of elasticity. The elastic stiffness of material depends on the porosity of coatings. As the coating thickness increases, the porosity remarkable increases which also bring down elastic modulus[50]. Porosity and the bonding strength are highly affects the elastic modulus[51,52]. As compared to 150lm coating thickness, 450lm has less elastic modulus and high porous because of decrease in bonding. The decrease in adhesive strength of the coating is noticed with the increase in the thickness limited to 7%[49].

10. Erosion rate

Impact angle will be the function of variation in slurry erosion rate with different coating thickness as shown in Figure 6. The increase in impact angle (30° to 90°) exhibits an increase in slurry erosion rate, again the magnitude is different for different coatings. The coating of 450lm has revealed 56% raise in erosion rate by the change in impact angle from 30° to 90° and similar results observed for 300ml[49].

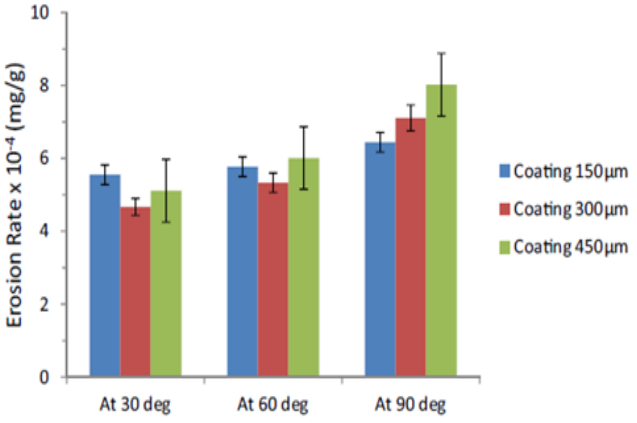


Figure 6. Results of Erosion wear of WC-10Co-4Cr composite coating[48].

Table 5. HVOF coating parameters[16]

O_2	850 l/min
Kerosene	22.5 l/h
lambda	1.1
Ar	2 x 11 l/min
Nozzle	100/12
Powder feed rate	2x35 g/min
Spraying distance	360 mm
Relative traverse speed	1.0 m/s
Spray path offset	5 mm

Lobel *et al.*[16] used inert gas atomization process in feedstock powder of AlCoCrFeNiTi0.5 for the HVOF spray coating. The powder fraction of −45+15 µm was used for the coating process, which was sorted by air. A backscattered electron detector was used for investigation. Typical images of powder fractions are shown in Figure 7. Atomized spherical powder particles are observed[16].

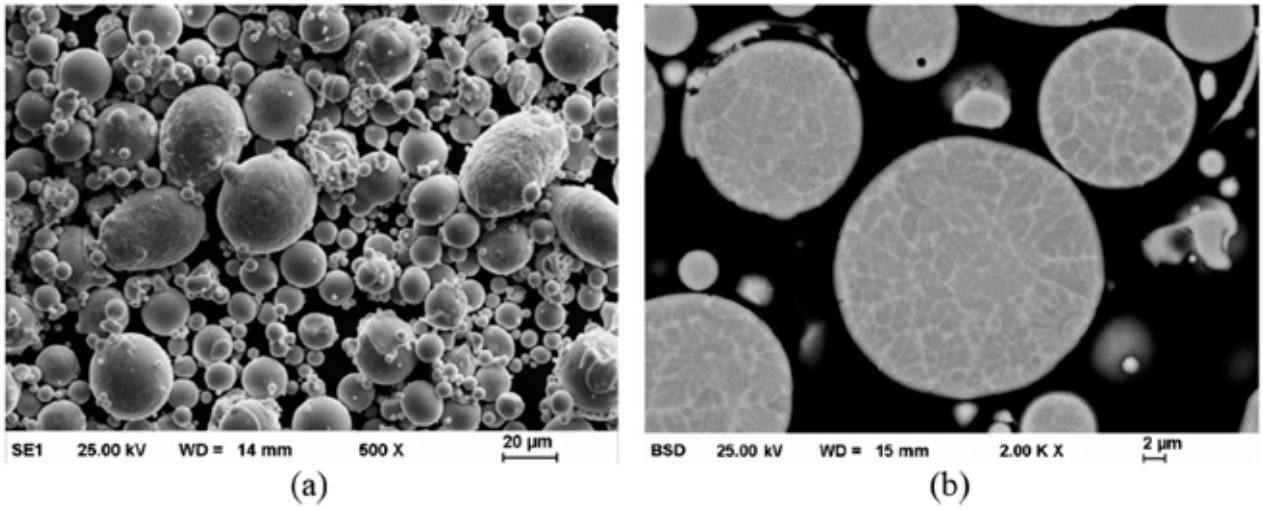


Figure 7. Gas atomized $AlCoCrFeNiTi_{0.5}$ composite powder images: **(a)** surface and **(b)** cross-section[16].

Table 5 provides the details of HVOF coating parameters used.

11.0 Wear investigations

Tests under reciprocating wear conditions show that the wear depth certainly dependent on test temperature in HVOF coatings. The negligible increase in wear depth is noticed by increasing room temperature to 500°C, and consequently, a decrease in wear resistance takes place. This action may be due to the thermal softening effect. An additional increase in temperature affects a decrease in wear depth. The lowest value of wear depth was noticed at a temperature of 900°C. With increasing temperature, the co-efficient of friction primarily increases. The coefficient of friction decreases as the temperature increased more than 650°C. The lowest average co-efficient of friction of 0.97 was noticed for the test results at higher temperature limit at 900°C shown in Figure 8[16].

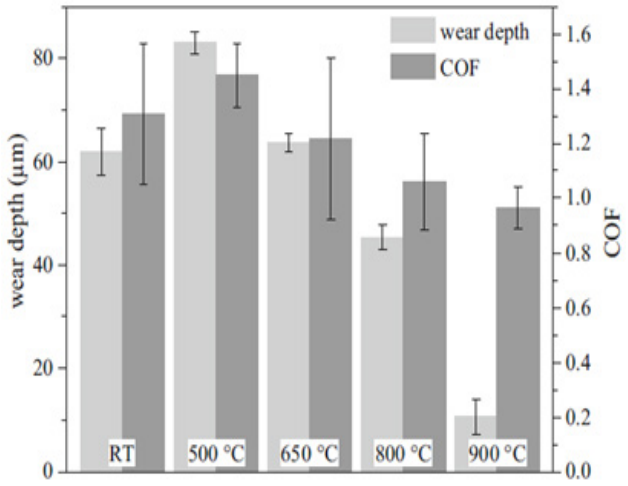


Figure 8. Wear depth and coefficient of friction tested under various temperatures using reciprocating method[16].

Wang *et al.*[40] used more than 99.5% pure TiB_2-50Ni powder was utilized for the HVOF coating process with different parameters shown in Table 6. An electrolysis-plated Ni film was homogeneously deposited on the surface of the ceramic element, and then a unique "Core-Shell" feedstock was prepared. The TiB_2 segment was separated from the air by Ni film while carrying coating by the HVOF process. The combination between TiB2 and Ni particles can enhance the superior adhesion of metal with an average particle size (APS) of 45 μm, which is suitably used for the HVOF coating process.

12.0 Microstructure and Phase Constituents

Very fewer micro pores and unmelted constituent parts were noticed in the lamellar structure cross section shown in Figure 9(a). About 300 μm average coating thickness possible by using HVOF spray process. Figure 9(b) is a detailed enlarged image of A in Figure 9(a). Figure 9(b) shows lamellar and granular morphologies characterized by dark gray phase. The coating top surface is almost plain noticed in Figure 9(c). Figure 9(d) is a detailed enlargement of region B in Figure 9(c). The maximum amount of powder particles is completely melted, and distribution is observed in Figure 9 (d). The porosity of about 2.3%, micro-hardness of about 766.1 HV, surface roughness 2.3μm and average bonding strength of about 22.6 MPa were characterized in HVOF composite coating[40].

13.0 Friction and Wear Performance

At different friction temperatures, Figure 10(a) shows friction results of substrate without coating and Figure 10(b) shows TiB2-50Ni coating. The related ambient

Table 6. Parameters of HVOF spraying[40]

Parameters of HVOF spraying						
HVOF parameters	O_2 flow rate (Lh^{-1})	Carrier gas pressure MPa	Carrier gas flow rate ($Lmin^{-1}$)	Fuel flow rate (Lh^{-1})	Spray distance mm	Powder feed rate ($gmin^{-1}$)
Value	45	0.2	12	22	300	80

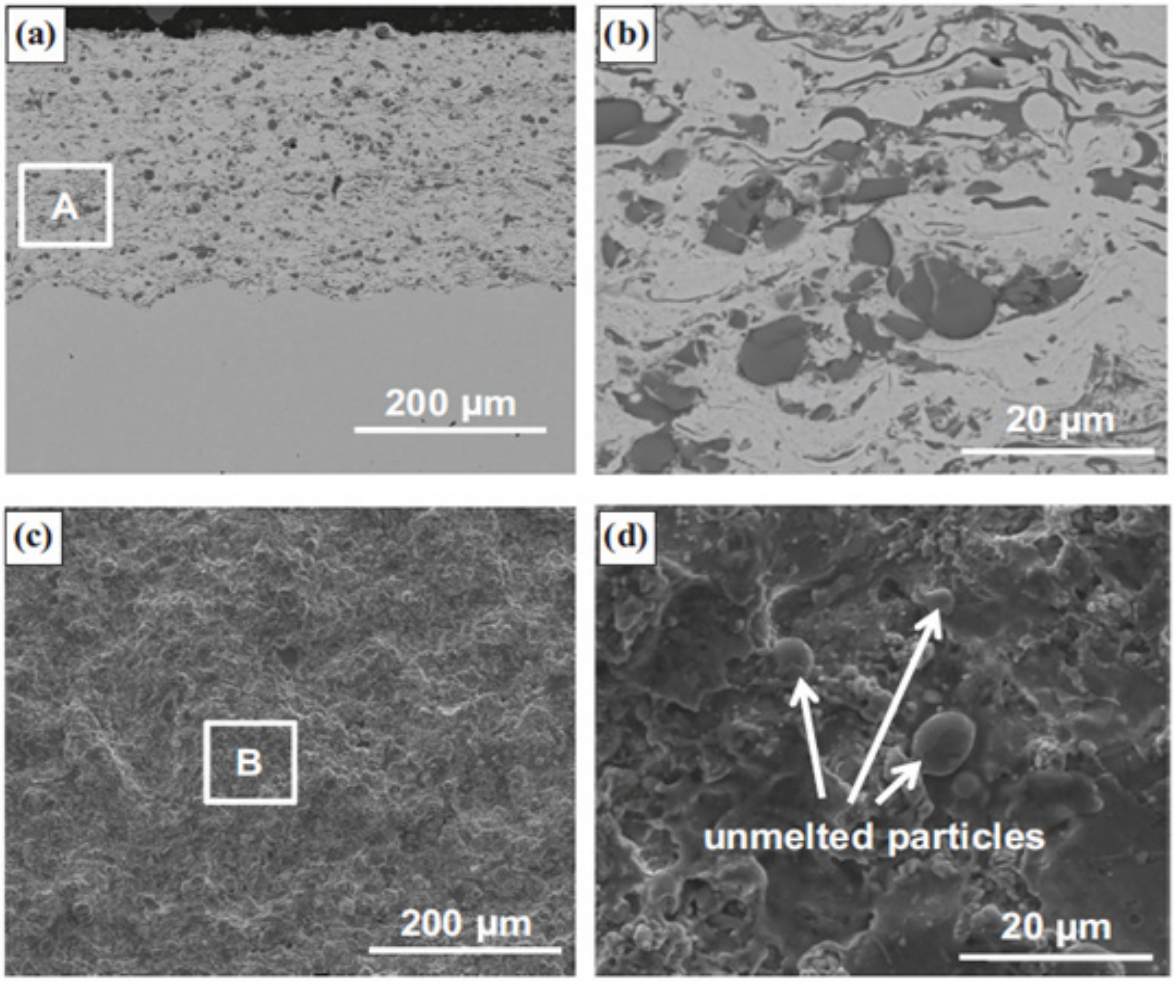


Figure 9. SEM morphologies of TiB_2-50Ni coating: **(a)** landscape of cross section, **(b)** detailed image of A in (a); **(c)** landscape of surface, **(d)** detailed image of B in (c)[40].

Table 7. Experimental parameters of wear test[40].

Sample No.	Temperature (°C)	Rotation Radius (mm)	Rotation Speed (r/min)	Load (N)	Wear Time (min)	Room Temperature Humidity (%)
1	23	1	300	20	30	80
2	150	1	300	20	30	80
3	300	1	300	20	30	80
4	450	1	300	20	30	80
5	600	1	300	20	30	80

temperatures are A-room temperature, B-150°C, C-300°C, D-450°C and E-600°C having friction coefficients 0.17 ± 0.02, 0.24 ± 0.03, 0.42 ± 0.04, 0.31 ± 0.03 and 0.35± 0.02, for 304 stainless steel substrate and 0.32 ± 0.01, 0.33 ± 0.01, 0.37 ± 0.01, 0.31 ± 0.01 and 0.37± 0.01, for HVOF TiB_2-50Ni coating respectively (Table 7). The above

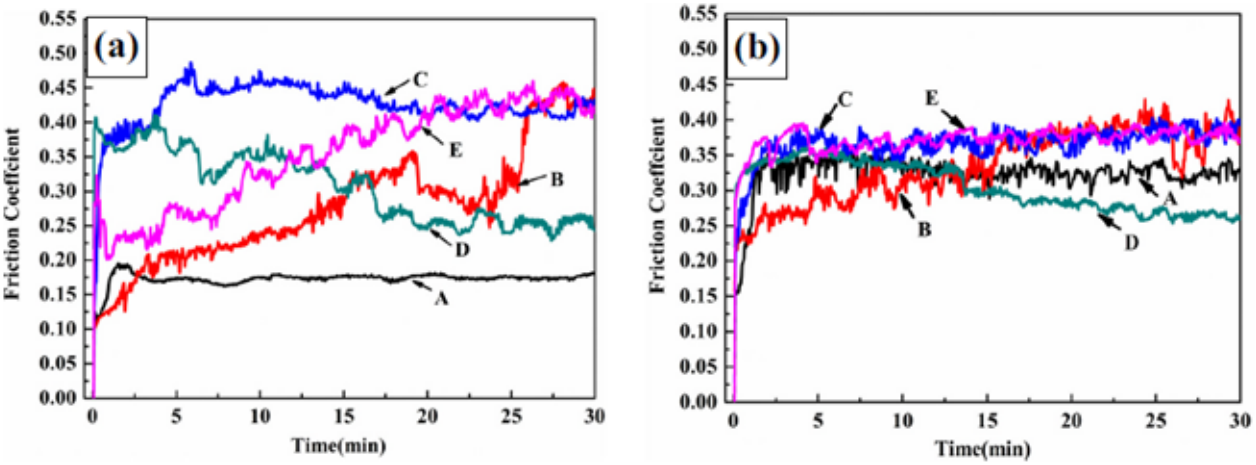


Figure 10. Friction coefficient curves at various temperatures **(a)** SS(304); **(b)** TiB_2-50Ni HVOF coating[40].

results and curves show better results for substrates with TiB_2-50Ni coating[40].

Ghadami *et al.*[30] The NiCoCrAIY powder produced by the gas atomization method was used as the feedstock material. In addition, CeO_2 (cerium oxide-99.99% purity) nanopowder was added as feedstock powder. Mild steel (0.23% C by weight) was used as substrates. Table 9 shows the characteristics of feedstock powder. A planetary rotating ball mill is used to blend NiCoCrAlY and CeO_2 nano composite particles. Three proportions, 0.5, 1 and 2 % by weight, were dry-ball milled. Stainless steel balls are coated by hard chrome plate and are used as a milling medium for about 25 hours.

Table 9. Characteristics of feedstock powder[23].

Characteristics	**NiCoCrAlY**	**Nano-CeO_2**
Powder size	-45 ± 5 (μm)	≥75 (nm)
Manufacturing process	Gas atomized	-
Product code	AMDRY 365-1	544841
Powder morphology	Spheroidal	Irregular
Manufacturing company	Oerlikon — Metco	Sigma-Aldrich

14.0 Coatings Characterization

The cross-sectional microstructure of thermally coated nanocomposite (NiCoCrAlY) coating with different values of reinforcement element of nano-CeO_2 are observed in Figure 11. It illustrates major phases with inter lamellar pore sand micro porosities and shows NiCoCr with solid-γ and NiAl-β lamellar structure. Significant quantities of oxides were observed with black regions at the boundary edge between splats noticed in Figure 11(a). Un-melted particles and micro porosities were also noticed in the regular NiCoCrAlY composite coating[30].

15.0 Micro Hardness

The results investigated are found from FESEM micrographs shown in Figure 11(a)-(d) with proportion of 0.5%, 1% and 2% by weight of nano-CeO_2 reinforcements. Figure 12 reveals lower porosity results with higher hardness for NiCoCrAlY/0.1CeO_2 in comparison with another type of regular and nanocomposite coatings. Hence NiCoCrAlY with 1% of nano-CeO_2 was chosen for practical applications with reference to the corresponding properties of regular NiCoCrAlY composite coatings[30].

Abu-warda *et al*[35] studied on the substrate SS(304) having dimensions 30mm×29mm×5 mm with ground surface (120 grit). The samples were ultrasonically cleaned

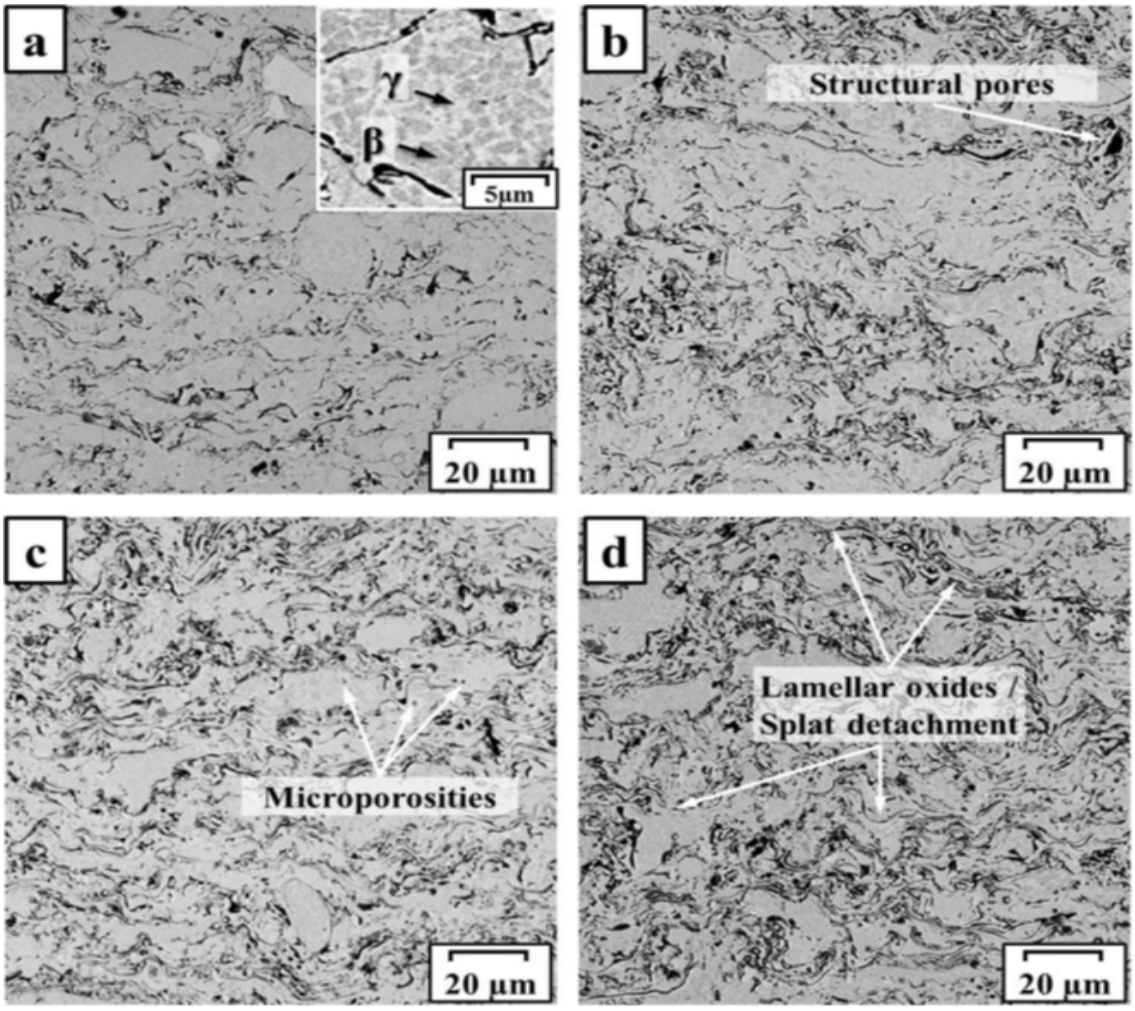


Figure 11. Micrographs of backscattered FESEM images **(a)** Regular NiCoCrAlY, and CeO_2 reinforced NiCoCrAlY **(b)** 0.5% by weight; **(c)** 1% by weight; d) 2% by weight of nanoCeO_2[23].

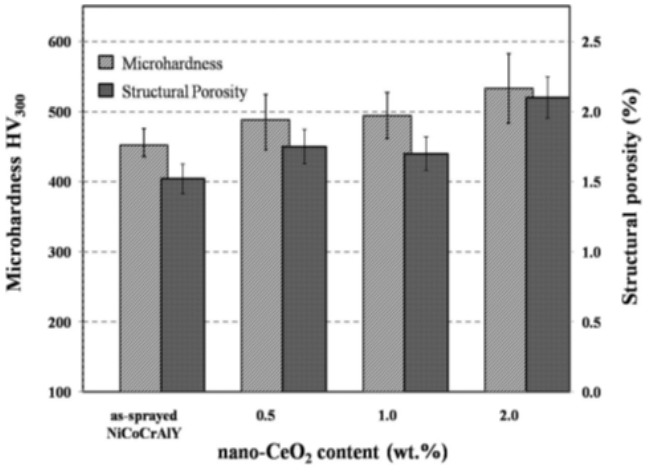


Figure 12. NiCoCrAlY composite with various proportions of CeO_2 coating graphs shows microhardness and porosity values[23].

prior to conducting tests at high temperature corrosion. Earlier to carry the deposition, the surface roughness is increased by sandblasting process with alumina particles (1mm average size) which increases the bonding strength of substrate with coating. Feedstock Al_2O_3-30Ni20Al cermet fine particles used. The NiAl powder particles were produced by chemical cladding, and they exist in spherical morphology, whereas Al_2O_3 particles were produced by crushing mechanically.

The study noticed that the initial properties and composition of the coating materials do not alter after HVOF method of deposition, and the presence of equal peaks found in feedstock powder Figure 13(a). The morphology of the coating has been analyzed by SEM and shown in Figure 13(b–c). 150 µm means coating thickness with irregular surface morphology was noticed, Figure

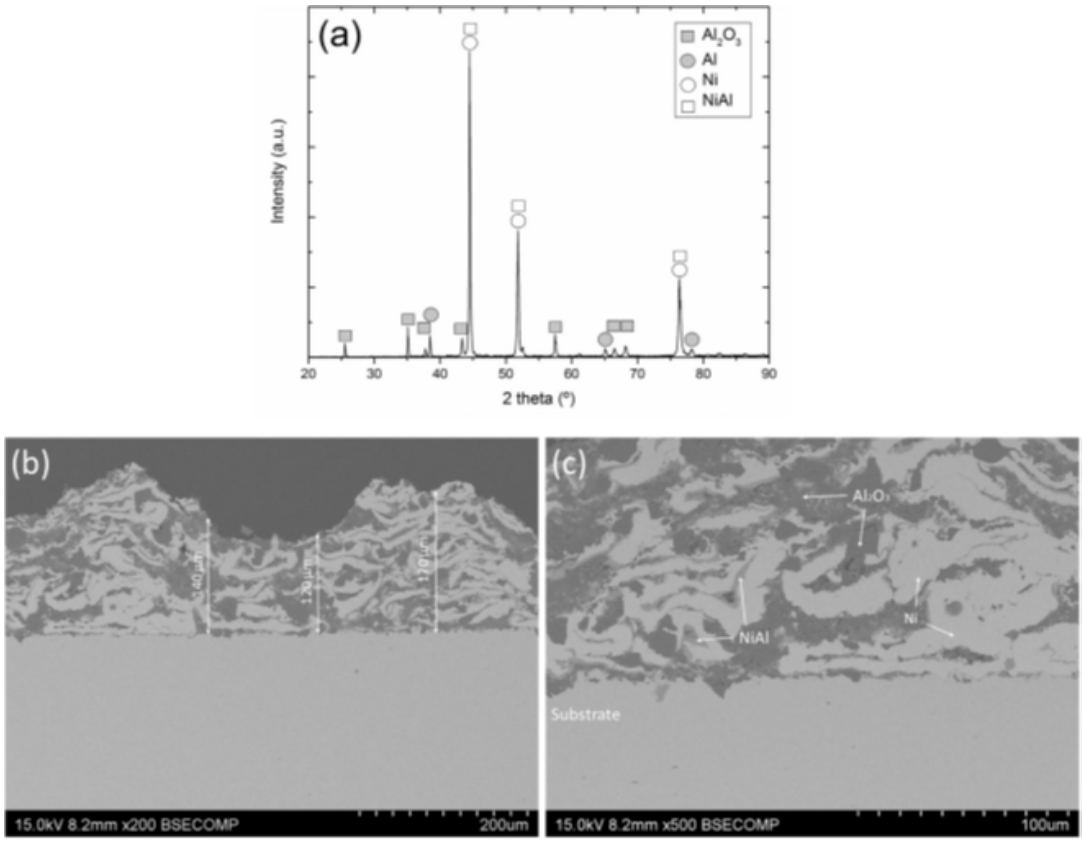


Figure 13. Characterization Al_2O_3-NiAl composite coating: **(a)** XRD and backscattered SEM **(b)** at X200 magnification and **(c)** at X500 magnification[35].

13(b). The metallic regions greatly Ni and ceramic regions Al_2O_3 phases were clearly observed Figure 13(b). As the shape of the coating is irregular, different deposited layers are difficult to identify. The coating has a smaller number of defects and shows good coating adhesion. The porosity is less than 2% volume in the coating therefore finishing treatments are not necessary. Better stress transformation takes place between metallic and ceramic phases due to the nonexistence of porosity in the boundaries[53]. This may enhance resistance to wear and minimize the particles separation from the coating during the wear test. Additionally, high ceramic particles deposition (86%) achieved because of melting temperatures difference in between metallic and ceramic particles[35].

16.0 Conclusions

- Uniform consistent coating is produced with the HVOF thermal spray coating.
- HVOF coating is suitable to have relative motion mating parts with alumina, silicon nitride as counter materials.
- Abrasion wear, splat spalling, microcracks, craters, ploughing are found as wear mechanisms.
- Nanostructured HVOF coated parts possess higher average hardness.
- The Ra results found to be higher for the worn surface and increase in wear rate with increase in temperature.
- The variation in mechanical properties and structural coatings resulted by the change in coating thickness.
- All the coated surfaces give brittle erosion for any value of coating thickness.
- Development of tribo-film on the worn surface was recognized and it helps to minimize friction and wear.

- The main characteristic feature of nanocomposite coatings is the development of adhesive protective oxide-layer with no crack indications.
- The study exposed good-adhered, dense, defects free coating. Importantly the substrate properties were not damaged after the coating.

17.0 References

1. Vats A, Kumar A, Patnaik A, Meena ML. Influence of deposition parameters on Tribological Performance of HVOF Coating: A review. In: IOP Conference Series: Materials Science and Engineering. IOP Publishing Ltd; 2021. https://doi.org/10.1088/1757-899X/1017/1/012015
2. Vashishtha N, Khatirkar RK, Sapate SG. Tribological behaviour of HVOF sprayed WC-12Co, WC-10Co-4Cr and Cr3C2–25NiCr coatings. Tribol Int. 2017; 105:55-68. https://doi.org/10.1016/j.triboint.2016.09.025
3. Hong S, Wu Y, Wang B, Zhang J, Zheng Y, Qiao L. The effect of temperature on the dry sliding wear behavior of HVOF sprayed nanostructured WC-CoCr coatings. Ceram Int. 2017; 43:458-462. https://doi.org/10.1016/j.ceramint.2016.09.180
4. Fotovvati B, Namdari N, Dehghanghadikolaei A. On coating techniques for surface protection: A review. J Manuf Mater Process. 2019; 3(1). https://doi.org/10.3390/jmmp3010028
5. Dehghanghadikolaei A, Mohammadian B, Namdari N, Fotovvati B. Abrasive machining techniques for biomedical device applications. JOJ Material Sci. n.d. https://doi.org/10.19080/JOJMS.2018.04.555653
6. Li CJ, Luo XT, Dong XY, Zhang L, Li CX. Recent research advances in plasma spraying of bulk-like dense metal coatings with metallurgically bonded lamellae. J Therm Spray Technol. 2022; 31:5-27. https://doi.org/10.1007/s11666-022-01327-x
7. Berghaus O. The 2016 Thermal spray roadmap. J Therm Spray Technol. 2016; 25:1376-1440. https://doi.org/10.1007/s11666-016-0473-x
8. Raza A, Ahmad F, Badri TM, Raza MR, Malik K. An Influence of oxygen flow rate and spray distance on the porosity of HVOF coating and its effects on corrosion-A review. Materials (Basel). 2022; 15(18). https://doi.org/10.3390/ma15186329
9. Sampath S, Jiang XY, Matejicek J, Prchlik L, Kulkarni A, Vaidya A. Role of thermal spray processing method on the microstructure, residual stress and properties of coatings: An integrated study of Ni-5 wt.% Al bond coats. Mater Sci Eng A. 2004; 364:216-231. https://doi.org/10.1016/j.msea.2003.08.023
10. Cizek J, Matejicek J. Medicine meets thermal spray technology: A review of patents. J Therm Spray Technol. 2018; 27:1251-1279. https://doi.org/10.1007/s11666-018-0798-8
11. Al-mutairi S, Hashmi MSJ, Yilbas BS, Stokes J. Microstructural characterization of HVOF/plasma thermal spray of micro/nano WC-12% Co powders. Surf Coat Technol. 2015; 264:175-186. https://doi.org/10.1016/j.surfcoat.2014.12.050
12. Lekatou A, Sioulas D, Karantzalis AE, Grimanelis D. A comparative study on the microstructure and surface property evaluation of coatings produced from nanostructured and conventional WC-Co powders HVOF-sprayed on Al7075. Surf Coat Technol. 2015; 276:539-556. https://doi.org/10.1016/j.surfcoat.2015.06.017
13. Wang H, Song X, Wang X, Liu X, Wang X. Fabrication of nanostructured WC-Co coating with low decarburization. Int J Refract Met Hard Mater. 2015; 53:92-97. Available from: https://doi.org/10.1016/j.ijrmhm.2015.05.010
14. Jafari M, Enayati MH, Salehi M, Nahvi SM, Han JC, Park CG. High temperature oxidation behavior of micro/nanostructured WC-Co coatings deposited from Ni-coated powders using high velocity oxygen fuel spraying. Surf Coat Technol. 2016; 302:426-437. https://doi.org/10.1016/j.surfcoat.2016.06.044
15. Oksa M, Turunen E, Suhonen T, Varis T, Hannula S. Optimization and characterization of high velocity oxy-fuel sprayed coatings: Techniques, materials, and applications. Coatings. 2011; 1(1):17-52. https://doi.org/10.3390/coatings1010017
16. Löbel M, Lindner T, Lampke T. High-temperature wear behaviour of AlCoCrFeNiTi0.5 coatings produced by HVOF. Surf Coatings Technol. 2020; 403. https://doi.org/10.1016/j.surfcoat.2020.126379
17. Thomas L, Rymer ML, Lo M, Bjo S. Microstructure and corrosion properties of alcrfeconi high-entropy alloy coatings prepared by HVAF and HVOF. J Therm Spray Technol. 2022; 247-255. https://doi.org/10.1007/s11666-021-01255-2
18. Pishva P, Salehi M, Golozar MA. Effect of grinding on surface characteristics of HVOF-sprayed WC-10Co-4Cr coatings. Surf Eng. 2020; 36:1180-1189. https://doi.org/10.1080/02670844.2019.1647938

19. Rukhande SW, Rathod WS, Bhosale DG. Dry sliding wear behaviour of HVOF sprayed NiCrBSiFe coating on SS 316L. In: Materials Today Proceedings. Elsevier Ltd; 2020. p. 765-71. https://doi.org/10.1016/j.matpr.2020.08.408
20. Rukhande S, Rathod WS, Bhosale D. Tribological behaviour of thermally sprayed coatings: A review. 2018. https://doi.org/10.2139/ssrn.3323697
21. Bolelli G, Berger LM, Börner T, Koivuluoto H, Matikainen V, Lusvarghi L, *et al*. Sliding and abrasive wear behaviour of HVOF- and HVAF-sprayed Cr3C2-NiCr hardmetal coatings. Wear. 2016; 358-59:32-50. https://doi.org/10.1016/j.wear.2016.03.034
22. Derelizade K, Rincon A, Venturi F, Wellman RG, Kholobystov A, Hussain T. High temperature (900 °C) sliding wear of CrNiAlCY coatings deposited by high velocity oxy fuel thermal spray. Surf Coatings Technol. 2022; 432. https://doi.org/10.1016/j.surfcoat.2021.128063
23. Nieto A, Kim J, Penkov OV. Elevated temperature wear behavior of thermally sprayed WC-Co/nanodiamond composite coatings. (n.d.):1-37.
24. Liu Y, Cheng J, Yin B, Zhu S, Qiao Z, Yang J. Study of the tribological behaviors and wear mechanisms of WC-Co and WC-Fe_3Al hard materials under dry sliding condition. Tribol Int. 2017; 109:19-25. https://doi.org/10.1016/j.triboint.2016.12.023.
25. Dejun K, Tianyuan S. Wear behaviors of HVOF sprayed WC-12Co coatings by laser remelting under lubricated condition. Opt Laser Technol. 2017; 89:86-91. https://doi.org/10.1016/j.optlastec.2016.09.043
26. Wang H, Wang X, Song X, Liu X, Liu X. Sliding wear behavior of nanostructured WC-Co-Cr coatings. Appl Surf Sci. 2015; 355:453-60. https://doi.org/10.1016/j.apsusc.2015.07.144
27. Ma N, Guo L, Cheng Z, Wu H, Ye F, Zhang K. Improvement on mechanical properties and wear resistance of HVOF sprayed WC-12Co coatings by optimizing feedstock structure. Appl Surf Sci. 2014; 320:364-71. https://doi.org/10.1016/j.apsusc.2014.09.081
28. Mi P, Wang T, Ye F. Influences of the compositions and mechanical properties of HVOF sprayed bimodal WC-Co coating on its high-temperature wear performance. Int J Refract Met Hard Mater. 2017; 69:158-63. https://doi.org/10.1016/j.ijrmhm.2017.08.012
29. Wang Q, Chen Z, Li L, Yang G. The parameters optimization and abrasion wear mechanism of liquid fuel HVOF sprayed bimodal WC-12Co coating. Surf Coat Technol. 2012; 206:2233-41. https://doi.org/10.1016/j.surfcoat.2011.09.071
30. Ghadami F, Zakeri A, Aghdam ASR, Tahmasebi R. Structural characteristics and high-temperature oxidation behavior of HVOF sprayed nano-CeO_2 reinforced NiCoCrAlY nanocomposite coatings. Surf Coat Technol. 2019; 373:7-16. https://doi.org/10.1016/j.surfcoat.2019.05.062
31. Achar DRG, Singheiser L, Quadakkers WJ. Modelling of phase equilibria in MCrAlY coating systems. Surf Coat Technol. 2004; 187:272-83. https://doi.org/10.1016/j.surfcoat.2004.02.018
32. Strauss D, Muller G. Oxide scale growth on MCrAlY bond coatings after pulsed electron beam treatment and deposition of EBPVD-TBC. Surf Coat Technol. 2001; 146:196-201. https://doi.org/10.1016/S0257-8972(00)00916-6
33. Mercier D, Gauntt BD, Brochu M. Thermal stability and oxidation behavior of nanostructured NiCoCrAlY coatings. Surf Coat Technol. 2011; 205:4162-68. https://doi.org/10.1016/j.surfcoat.2011.03.005
34. Saeedi B, Aghdam ASR, Gholami G. A study on nanostructured in-situ oxide dispersed NiAl coating and its high-temperature oxidation behavior. Surf Coat Technol. 2015; 276:704-13. https://doi.org/10.1016/j.surfcoat.2015.05.042.
35. Abu-warda N, López MD, Utrilla MV. High-temperature corrosion and wear behavior of HVOF-sprayed coating of Al_2O_3-NiAl on AISI 304 stainless steel. Surf Coat Technol. 2019; 359:35-46. https://doi.org/10.1016/j.surfcoat.2018.12.047.
36. Khan J, Arsalan MH. Solar power technologies for sustainable electricity generation- A review. Renew Sustain Energy Rev. 2016; 55:414-25. https://doi.org/10.1016/j.rser.2015.10.135.
37. Drane PJ, Hansen CJ, Inalpolat M, Mack JH, Myers AT, Rotea M. Wind energy research: State-of-the-Art. Renew Energy. 2018. https://doi.org/10.1016/j.renene.2018.02.049
38. Wang B, Lee SW. Erosion-corrosion behavior of HVOF NiAl-Al_2O_3 intermetallic-ceramic coating. Wear. 2000; 239:83-90. https://doi.org/10.1016/S0043-1648(00)00309-4
39. Liu S, Zhang W. Research on microstructure of in situ synthesized TiB_2/Ni metal-ceramics composite coating. J Alloys Compd. 2005; 391:146-50. https://doi.org/10.1016/j.jallcom.2004.07.078.
40. Wang Y, Zhang W, Chen D, Liu X, Hu W, Liu L, *et al*. High-temperature friction and wear performance

of TiB_2-50Ni composite coating sprayed by HVOF technique. Surf Coat Technol. 2021; 407. https://doi.org/10.1016/j.surfcoat.2020.126766

41. Oladijo OP, Sacks N, Cornish LA, Venter AM. Effect of substrate on the three-body abrasion wear of HVOF WC-17 wt.% Co coatings. Int J Refract Met Hard Mater. 2012; 35:288-94. https://doi.org/10.1016/j.ijrmhm.2012.06.011
42. Hong S, Wu Y, Wang Q, Ying G, Li G, Gao W, *et al*. Microstructure and cavitation-silt erosion behavior of high-velocity oxygen-fuel (HVOF) sprayed Cr_3C_2-NiCr coating. Surf Coat Technol. 2013; 225:85-91. https://doi.org/10.1016/j.surfcoat.2013.03.020.
43. Zhu HB, Li H, Li ZX. Plasma sprayed TiB_2-Ni cermet coatings: Effect of feedstock characteristics on the microstructure and tribological performance. Surf Coat Technol. 2013; 235:620-27. https://doi.org/10.1016/j.surfcoat.2013.08.040
44. Qiao L, Wu Y, Hong S, Cheng J, Wei Z. Influence of the high-velocity oxygen-fuel spray parameters on the porosity and corrosion resistance of iron-based amorphous coatings. Surf Coat Technol. 2019; 366:296-302. https://doi.org/10.1016/j.surfcoat.2019.03.046
45. Vignesh S, Shanmugam K, Balasubramanian V, Sridhar K. Identifying the optimal HVOF spray parameters to attain minimum porosity and maximum hardness in iron-based amorphous metallic coatings. Def Technol. 2017; 13:101-10. https://doi.org/10.1016/j.dt.2017.03.001
46. Khosravifard A, Salahinejad E, Yaghtin AH, Araghi A, Akhbarizadeh A. Tribochemical behavior of alumina coatings deposited by high-velocity oxy fuel spraying. Ceram Int. 2015; 41(5):5713-20. https://doi.org/10.1016/j.ceramint.2015.01.002
47. Wojciech Ż. Tribological properties of plasma and HVOF-sprayed NiCrBSi-Fe_2O_3 composite coatings. Surf Coat Technol. 2013; 220:282-9. https://doi.org/10.1016/j.surfcoat.2012.09.057.
48. Cheng JB, Liang XB, Wang ZH, Xu BS. Dry sliding friction and wear properties of metallic glass coating and martensite stainless coating. Tribol Int. 2013; 60:140-6. https://doi.org/10.1016/j.triboint.2012.11.010
49. Sapate SG, Tangselwar N, Paul SN, Rathod RC, Mehar S, Gowtam DS, *et al*. Effect of coating thickness on the slurry erosion resistance of HVOF-sprayed WC-10Co-4Cr coatings. J Therm Spray Technol. 2021; 30(5):1365-79. https://doi.org/10.1007/s11666-021-01190-2
50. Taylor P, Li C, Ohmori A, Tani K. Effect of WC particle size on the abrasive wear of thermally sprayed WC-Co coatings. J Therm Spray Technol. (n.d.). https://doi.org/10.1080/10426919908914815
51. Taylor P, Usmani S, Sampath S, Houck DL, Lee D, Brook S, *et al*. Effect of carbide grain size on the sliding and abrasive wear behavior of thermally sprayed WC-Co coatings. Wear. (n.d.);37-41. https://doi.org/10.1080/10402009708983682
52. Ma K, Zhu J, Xie H, Wang H. Effect of porous microstructure on the elastic modulus of plasma-sprayed thermal barrier coatings: Experiment and numerical analysis. Surf Coat Technol. 2013; 235:589-95. https://doi.org/10.1016/j.surfcoat.2013.08.030
53. Zhang S, Cho T, Yoon J, Fang W, Song K, Li M, *et al*. Characterization of microstructure and surface properties of hybrid coatings of WC-CoCr prepared by laseinr heat treatment and high-velocity oxygen fuel spraying. Mater Charact. 2008; 9(1):3-9. https://doi.org/10.1016/j.matchar.2008.01.003